

Dynamic Contact Analysis of Laminated Composite Plates Under Low-Velocity Impact

Nam Seo Goo* and Seung Jo Kim†
Seoul National University, Seoul, 151-742, Republic of Korea

Simple laws, such as the modified Hertz contact law, have been used to impose the dynamic contact condition of composite laminates. However, these laws cannot account for span or thickness and stacking sequence of the laminate when simulating the dynamic contact behaviors. Special attention is given to the dynamic contact analysis of composite laminates under low-velocity impact as a precise method that can consider such parameters. To simulate the dynamic behaviors of composite laminates by a rigid impactor, three-dimensional finite element analysis is carried out. A formulation of the dynamic contact problem using the penalty finite element method is summarized. For the static case, the contact force-indentation relations for composite plates are investigated to reveal the contact behavior of composite plates and to point out the limitations of the modified Hertz contact law. For the dynamic case, impact forces of a composite laminate predicted by the present method are compared with the one by the modified Hertz contact law. Finally, impact behaviors of curved composite laminates, which are important in real applications, are investigated. Impact force histories of curved composite laminates with various curvatures and stacking sequences are presented. The results are compared with those of plates with the same dimensions and stacking sequences. The effects of curvature on impact response of composite laminates are presented.

Introduction

GENERALLY, impact responses of composite laminates can be described by solutions of dynamic contact problems. However, simpler methods have been used in most of the previous works. The Hertz indentation law, which is a quasistatic contact force-indentation relation, has been generally used for isotropic materials.¹ For composite materials, spring-mass models, energy balance models, and assumed force models have been utilized as simplified methods to understand the qualitative features of impact event.² Yang and Sun³ revealed that both loading and reloading curves seem to follow the 1.5 power law and the unloading curves follow the 2.5 power law from the quasistatic indentation tests. This law, called the modified Hertz contact law, has been applied to the study of low-velocity impact by Tan and Sun⁴ and many other researchers. However, the law cannot account for important parameters, such as stacking sequence, span or thickness of the laminate, and friction.

Recently, Wu and Yen⁵ considered the effects of the material properties, stacking sequence, span and thickness of the plate, and indenter's size on the contact force-indentation relations and showed that the modified Hertz contact law underestimates the contact force for the same indentation and that contact force-indentation relations are irrelevant to stacking sequence. Kim and Goo⁶ concluded that impactor's shape has influences on the static and dynamic contact behaviors between a rigid elliptic impactor and a composite laminate by the penalty finite element method and that the modified Hertz contact law cannot account for thickness effects of a laminate.

Real structures such as a section of laminated aircraft wing may have curvature. Therefore, the study of impact behaviors of curved laminates is important in real applications. Some studies have been concerned with the impact behaviors of cylinders and cylindrical shells.⁷⁻¹³ Kapania and Stoumbos⁷ made a rigorous review of the impact responses of laminated shells.

In this study, three-dimensional dynamic contact analysis of the composite laminate is carried out as a three-dimensional extension of the previous work.⁶ A formulation of the dynamic contact

problem and its finite element approximation is introduced briefly. As for static results, contact force-indentation relations for composite plates are investigated to reveal the contact behaviors of composite plates and limitations of the modified Hertz contact law. For the dynamic case, the impact force histories of a composite plate by the present method are compared with the one by the modified Hertz contact law. Finally, impact force histories of curved composite laminates with various curvatures and stacking sequences are presented and are compared with those of plates with the same dimensions and stacking sequences. The curvature effects on impact behaviors of composite laminates are investigated.

Governing Equations

For completeness, this part is introduced from previous work.⁶

Consider an elastic body Ω with a boundary Γ impacted by a rigid body R . This situation can be described by the following governing equations and constraint equations:

$$\begin{aligned} \rho \ddot{\mathbf{u}} - \nabla \cdot \boldsymbol{\sigma} &= \mathbf{f} & \text{in } \Omega \\ \mathbf{u} &= \bar{\mathbf{u}} & \text{on } \Gamma_D \\ t &= \bar{t} & \text{on } \Gamma_F \end{aligned} \quad (1)$$

and

$$\begin{aligned} u_n &\leq s, & \sigma_n &\leq 0 \\ \sigma_n(u_n - s) &= 0 & \text{on } \Gamma_C \\ \sigma_T &= 0 \end{aligned} \quad (2)$$

The initial condition is

$$\mathbf{u}(0) = \mathbf{u}_0, \quad \dot{\mathbf{u}}(0) = \dot{\mathbf{u}}_0 \quad (3)$$

where \mathbf{f} , \mathbf{u} , t , Γ_C , \mathbf{n} , and s are a body force, a displacement vector, a surface force, a candidate contact area, an outward normal vector on Γ_C and a contact gap, respectively; and

$$\sigma_n = \mathbf{n} \cdot \boldsymbol{\sigma} \cdot \mathbf{n}, \quad \sigma_T = \mathbf{n} \cdot \boldsymbol{\sigma} - \sigma_n \mathbf{n}, \quad u_n = \mathbf{u} \cdot \mathbf{n} \quad (4)$$

The strain-displacement relation is

$$\bar{\boldsymbol{\epsilon}} = \frac{1}{2} [\nabla \mathbf{u} + (\nabla \mathbf{u})^T] \quad (5)$$

where superscript T indicates transposition.

The constitutive relation is

$$\boldsymbol{\sigma} = \mathbf{D} \cdot \boldsymbol{\epsilon} \quad (6)$$

Received May 28, 1996; revision received March 18, 1997; accepted for publication May 5, 1997. Copyright © 1997 by the American Institute of Aeronautics and Astronautics, Inc. All rights reserved.

*Graduate Research Assistant, Department of Aerospace Engineering; currently Senior Researcher, Division 4-3-3, Agency for Defense Development, Daejeon 305-600, Republic of Korea. Member AIAA.

†Professor, Department of Aerospace Engineering. Member AIAA.

where $\varepsilon = [\varepsilon_{11}, \varepsilon_{22}, \varepsilon_{33}, \gamma_{23}, \gamma_{31}, \gamma_{12}]^T = [\bar{\varepsilon}_{11}, \bar{\varepsilon}_{22}, \bar{\varepsilon}_{33}, 2\bar{\varepsilon}_{23}, 2\bar{\varepsilon}_{31}, 2\bar{\varepsilon}_{12}]^T$ are constitutive relations of composite laminates.

There are mainly two approaches to solve inequality-constrained problems: the penalty method and the Lagrange multiplier method. We adopted a penalty method because it does not introduce any new degree of freedom as does the Lagrange multiplier method.

Using the exterior penalty method,¹⁴⁻¹⁷ the preceding equations can be written in the following variational form:

$$\int_{\Omega} \left[\int_{\Omega} \rho \ddot{u} \cdot \delta u \, d\Omega + \int_{\Omega} \sigma \cdot \delta \varepsilon \, d\Omega - \int_{\Omega} f \cdot \delta u \, d\Omega - \int_{\Gamma_F} \bar{t} \cdot \delta u \, dS + \frac{1}{\varepsilon} \int_{\Gamma_C} (u_n - s)^+ \mathbf{n} \cdot \delta u \, dS \right] dt = 0 \quad (7)$$

where $\psi^+(x) = \max\{\psi(x), 0\}$ is a nondifferentiable function at $x=0$ and ε is supposed to be a small number or a penalty parameter. The last term in the left-hand side of Eq. (7) makes the problem nonlinear. Then the normal stress on the contact boundary can be obtained as

$$\sigma_n = -(1/\varepsilon)(u_n - s)^+ \quad (8)$$

Rigid body dynamics is used for impactor. The contact force f between impactor and composite laminate can be sought by integrating the contact stress over the contact boundary Γ_C :

$$f = \int_{\Gamma_C} \sigma_n \mathbf{n} \cdot \mathbf{i}_Z \, dS \quad (9)$$

where \mathbf{i}_Z is the Z -direction base vector.

Numerical Procedure and Verification

Eight-node incompatible elements are used for finite element analysis. Incompatible modes are used to enhance the solution accuracy in solving the bending problems.¹⁸⁻²⁰ To pass the patch test, Taylor's modification¹⁸ is adopted. A successive iteration method¹⁵ is used to deal with nonlinearity, which comes from contact conditions. Relative error of displacement is used as a convergence criterion. Note that the Gauss integration of nonlinear stiffness matrix and force vector, \mathbf{K}_N and \mathbf{F}_N [see Eq. (21) in Ref. 21], leads to the numerical instability of the solution.²² Instead of the Gauss quadrature rule, the trapezoidal rule is adopted.

The discretized governing equations is integrated by the Newmark constant-average-acceleration method with $\beta = 0.5$ and $\gamma = 0.25$. To describe the dynamic contact phenomena between impactor and composite laminate, the equilibrium position of impactor and composite laminate must be determined for each time step. In this work the algorithm proposed in the preceding work⁶ is used.

Detailed finite element approximation and verifications of the developed numerical code can be found in Refs. 21 and 23. The following is presented as a typical example to verify the Hertzian contact behavior.

Consider a steel plate ($E = 210$ GPa, $\nu = 0.3$) indented by a rigid spherical indenter. The bottom of the plate is placed on a rigid support. The size of the plate is large enough to reproduce an infinite half-plane: $10 \times 10 \times 4$ cm and $R = 6.35$ mm. Therefore, the contact force f with respect to the indentation α can be determined by the elastic contact law given as

$$f = k\alpha^{3/2} \quad (10)$$

where the contact constant k_{iso} for isotropic material can be given as

$$k = k_{\text{iso}} = \frac{4}{3} \sqrt{R[E/(1-\nu^2)]}$$

where ν is the Poisson ratio of the plate and E is Young's modulus of the plate. R is the radius of the indenter.

For the finite element calculation, 900 ($15 \times 15 \times 4$) finite elements are used for a quarter of the plate. The predicted contact force was in excellent agreement with the Hertz contact law. (The result is not given in this paper.)

Results and Discussions

Contact Force-Indentation Relations

In this section, the effects of the lamination pattern on the contact force-indentation f - α relation of composite laminate are examined. The $50 \times 32 \times 2.7$ mm plate, which has the same dimension and boundary condition (fixed at two edges) as Yang and Sun's³ experiment, is selected. The lamination patterns of the plate are $[0_{20}]$, $[90_{20}]$, $[0_5/90_5]_s$, $[90_5/0_5]_s$, and $[45_5/-45_5]_s$. The lamination pattern in Yang and Sun's³ experiment is $[0/45/0/-45/0]_{2s}$. The mechanical properties are $E_1 = 120$ GPa, $E_2 = 7.9$ GPa, $G_{12} = 5.5$ GPa, and $\nu_{12} = \nu_{23} = 0.3$, and the radius of the indenter is $R = 6.35$ mm.

In the following discussions, the indentation α is defined as

$$\alpha = w(x_0, y_0, -h/2) - w(x_0, y_0, h/2) \quad (11)$$

where w is the vertical displacement of the plate, x_0, y_0 is the center point of contact, and h is the thickness of the plate.

For the finite element calculation, a total of 900 ($15 \times 15 \times 4$) finite elements is used for a quarter of the plate. Figure 1 shows the finite element calculation of contact force-indentation relation. From Fig. 1, it is observed that when the indentation is small, all lamination patterns, except $[45_5/-45_5]_s$, have similar f - α relations. In particular, $[0_{20}]$ and $[0_5/90_5]_s$ laminates have the same tendency. However, as the indentation increases, the f - α relation becomes different for different ply sequences. It can be concluded that the f - α relation of the composite plate is influenced by the lamination pattern, whereas Wu and Yen⁵ showed that the f - α relations were not influenced by the ply sequence.

Now let us investigate limitations of the modified Hertz contact law.

A $50 \times 32 \times 2.54$ mm plate made from T300/934 GFRP (graphite fiber reinforced plastic)²⁴ is considered. The mechanical properties of T300/934 GFRP are $E_1 = 145.4$ GPa, $E_2 = 9.997$ GPa, $G_{12} = 5.689$ GPa, and $\nu_{12} = \nu_{23} = 0.3$, and the radius of the indenter is $R = 6.35$ mm. Five ply sequences, $[0_{16}]$, $[90_{16}]$, $[0_4/90_4]_s$, $[90_4/0_4]_s$, and $[45_4/-45_4]_s$, are considered. The contact force-indentation relation given by the modified Hertz contact law is given by

$$k = k_{M-Hertz} = \frac{4}{3} \sqrt{RE_2} \quad (12)$$

where E_2 is Young's modulus in the transverse direction. In Fig. 2, the f - α relations of $[0_{16}]$, $[0_4/90_4]_s$, and $[90_4/0_4]_s$ are almost the same, and they are different from those of $[90_{16}]$ and $[45_4/-45_4]_s$.

Note that the modified Hertz contact law underestimates the contact force for the same indentation. This is because the Hertz contact

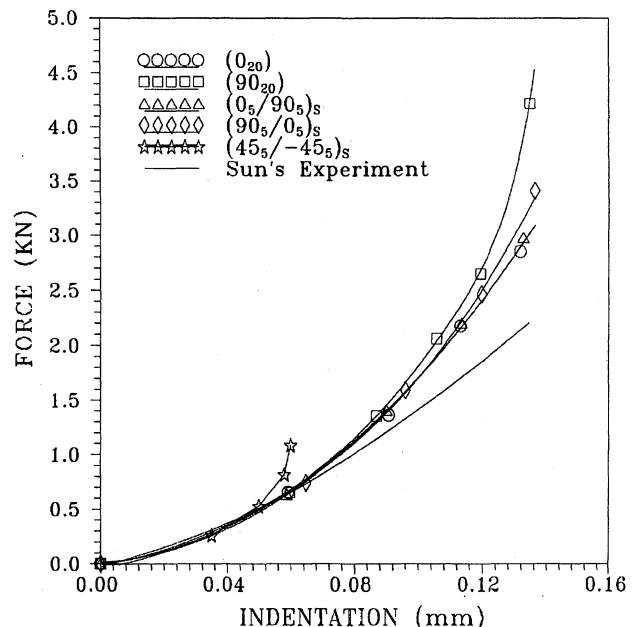


Fig. 1 Effect of lamination pattern on contact force-indentation relation of the composite plate used in Yang and Sun's experiment.³

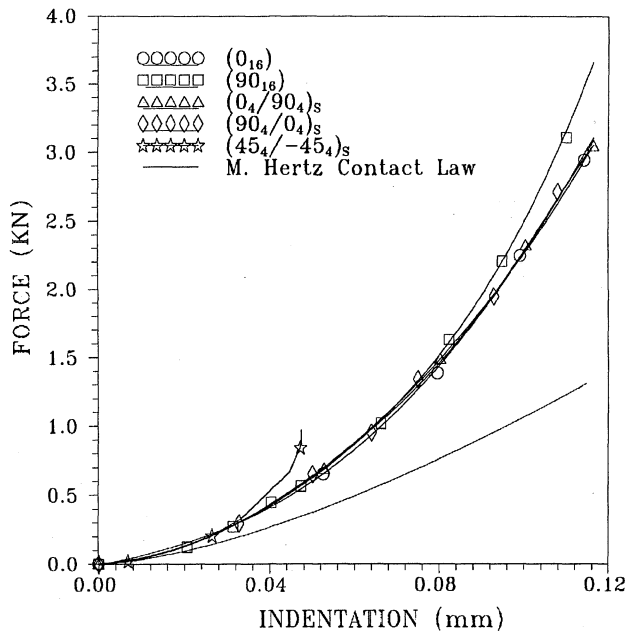


Fig. 2 Contact force-indentation relation of a T300/934 composite plate compared with the modified Hertz contact law.

law is derived from the infinite half-space and cannot account for the thickness effects.⁶ Also, note that the f - α relation by the modified Hertz contact law is independent of the lamination pattern.

Impact Responses of Flat and Curved Composite Laminates

In this section, two problems, penalty parameter convergency of impact response and comparison of the present result with the one using the modified Hertz contact law, are considered. Then, the impact responses of curved composite laminates are presented using dynamic contact analysis.

In general, the penalty parameter denotes the degree of constraint imposition on a system. Although the penalized solution approaches the exact solution for an infinitely small number of penalty parameters in the mathematical sense, it is observed that a small number of penalty parameters leads to numerical instability.^{25,26} Therefore, the penalty parameter ϵ must be an adequately small number so that the violation of the constraint is sufficiently penalized while ensuring that numerical instability does not occur. Roughly speaking, the penalty parameter of the present study can be determined by comparing an effective stiffness matrix and a nonlinear stiffness matrix [see Eq. (30) in Ref. 20]. In the first problem, an appropriate range of penalty parameters for the impact analysis is proposed by numerical experiment.

To this end, an 8×8 cm laminate with $[0_8/90_8]$ lamination pattern is used. The boundary condition is simply supported on all edges. The mass, velocity, and radius of impactor are 2.9 g, 5 m/s, and 6.35 mm, respectively. Again T300/934 GFRP is used, and the mechanical properties are as in the preceding section and $\rho = 1536 \text{ kg/m}^3$. A total of 450 ($15 \times 15 \times 2$) finite elements and a $1\text{-}\mu\text{s}$ time step size are used. Figure 3 shows the impact responses for five penalty parameters: 10^{-11} , 10^{-12} , 10^{-13} , 10^{-14} , and 10^{-15} . From the results, impact responses are converged for the penalty parameters less than 10^{-13} . The present algorithm is not sensitive to penalty parameter as long as it is less than 10^{-13} .

In the second problem, an impact response of the composite laminate by the present method is compared with the one using the modified Hertz contact law. A 10.16×7.62 cm laminate with $[0_3/90_5]_s$ lamination pattern is impacted by the impactor, whose mass and velocity are 0.16 kg and 3.38 m/s. The laminate is fixed at two edges. T300/976 GFRP is used. The mechanical properties are $E_1 = 156.0 \text{ GPa}$, $E_2 = 9.09 \text{ GPa}$, $G_{12} = 6.96 \text{ GPa}$, and $\nu_{12} = \nu_{23} = 0.4$, and the radius of the impactor is $R = 6.35 \text{ mm}$.

For the finite element calculation, only a quarter of the plate is considered (due to symmetry) and a total of 900 ($15 \times 15 \times 4$) finite elements and a $10\text{-}\mu\text{s}$ time step size are used. The penalty parameter is 10^{-13} . Impact responses using the present method and the three-

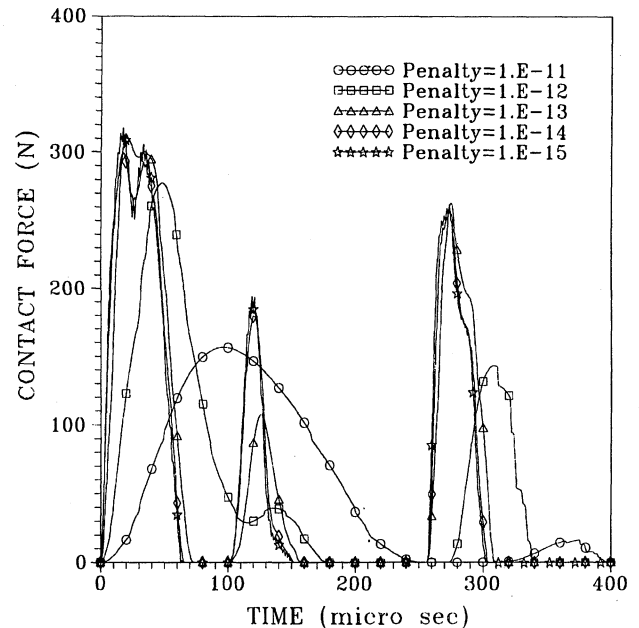


Fig. 3 Penalty parameter convergency: time vs impact force history of central transverse impact on a simply supported $[0_8/90_8]$ composite plate.

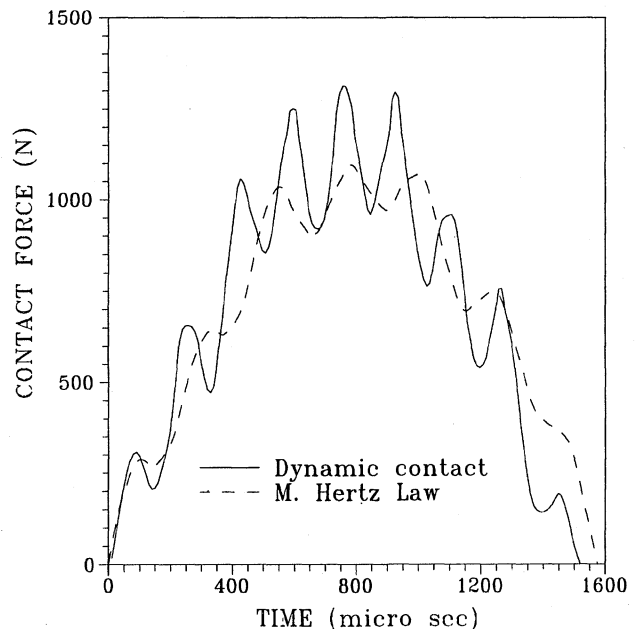


Fig. 4 Finite element calculation of the impact force of a T300/976 $[0_3/90_5]_s$ composite laminate due to low-velocity impact compared with the result using modified Hertz contact law.

dimensional finite element calculation in conjunction with modified Hertz contact law are given in Fig. 4. The result by the modified Hertz contact law is from our previous work.²⁷ There are two main reasons why the two results differ. The first is the limitation of the modified Hertz contact law. The modified Hertz contact law cannot account for the thickness and the ply layup effect; the impact force history obtained using the modified Hertz contact law, thus, may differ from the real situation. The second is the use of the quasistatic contact law. Recent work revealed that the quasistatic f - α relation (contact law) has some discrepancy with the dynamic f - α relation in predicting the impact force history of a composite plate.²⁸ This is due to the dynamic effect of the impact phenomenon, and it shows the limitation of the static contact law in impact analysis. We believe that three-dimensional dynamic contact analysis, which does not require a contact law, gives a better solution of the low-velocity impact problem, although the quasistatic contact law in conjunction with three-dimensional finite element or plate theory can predict the impact force history fairly accurately.

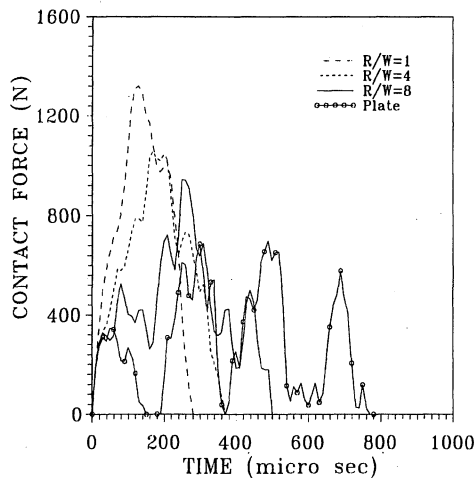


Fig. 5 Effect of curvature on time vs impact force history of a $[0_4/90_4/90_4/0_4]$ composite laminate impacted by an impactor: mass, 30 g and velocity, 15 m/s.

Finally, impact responses of curved composite laminates are investigated using the dynamic contact analysis.

For the numerical calculation, a cylindrical panel, whose projected shape is a square with the dimension length $L = \text{width } W = 8$ cm, is used. The four radii of curvature, $R/W = 1, 4, 8$, and ∞ (plate), are considered. The lamination pattern is $[0_4/90_4/90_4/0_4]$. The laminate is simply supported on all edges, and the velocity of an impactor is 15 m/s. The kinetic energy is 3.375 J. The mechanical properties of T300/934 GFRP are used, and the radius of the indenter is $R = 6.35$ mm. A quarter model with 900 ($15 \times 15 \times 4$) elements and a 5- μ s time step size are used.

Figure 5 shows the impact responses of the curved composite laminate according to the curvatures. As curvature decreases (or R/W increases), the responses return to those of the plate. However, for $R/W = 1$ and 4, the impact force history becomes different from that of the plate, or a single contact exists. As curvature increases, the maximum magnitudes of the contact forces become higher. From these results, it can be stated that the curved composite laminates demonstrate stiffer behavior than the plates, as physical intuition suggests.

Conclusions

The impact behaviors between a rigid impactor and a composite laminate are described by the solutions of the dynamic contact problem. The problem is solved by using the penalty finite element method. For time integration, the Newmark method is used, and for nonlinear analysis, the successive iteration method is adopted. An algorithm is used to determine the equilibrium position of a rigid impactor and a composite laminate at each time step. After verifying the developed code, static and dynamic contact behaviors of composite laminates are investigated. The relations of contact force and indentation of composite laminates are influenced by the lamination pattern. The modified Hertz contact law cannot account for the thickness effect and lamination patterns. But the present method can consider the thickness effect and lamination pattern, and it can be concluded that the dynamic contact analysis can describe the impact response of composite laminates more accurately. From the impact analysis of a curved composite laminate, it is noted that the impact forces of a curved composite laminate become higher as the curvature increases. Special attention must be given to the design and maintenance of structures made of curved composite laminates.

References

- ¹Goldsmith, W., *Impact*, Edward Arnold, Ltd., London, 1960.
- ²Abrate, S., "Impact on Laminated Composite Materials," *Applied Mechanics Reviews*, Vol. 44, No. 4, 1991, pp. 155–190.
- ³Yang, S. H., and Sun, C. T., "Indentation Law for Composite Laminates," *Composite Materials: Testing and Design (6th Conference)*, edited by I. M. Daniel, American Society for Testing and Materials, Philadelphia, PA, 1982, pp. 425–449 (ASTM STP 787).
- ⁴Tan, T. M., and Sun, C. T., "Use of Static Indentation Laws in the Impact

Analysis of Laminated Composite Plates," *Journal of Applied Mechanics*, Vol. 52, March 1985, pp. 5–12.

⁵Wu, E., and Yen, C., "The Contact Behavior Between Laminated Composite Plates and Rigid Spheres," *Journal of Applied Mechanics*, Vol. 61, March 1994, pp. 60–66.

⁶Kim, S. J., and Goo, N. S., "Dynamic Contact Responses of Laminated Composite Plates According to the Impactor's Shape," *Computers and Structures* (to be published).

⁷Kapania, R. K., and Stoumbos, T. G., "Geometrically Nonlinear Impact Response of Thin Laminated Imperfect Cylindrical Panels," *Composites Engineering*, Vol. 4, No. 4, 1994, pp. 397–416.

⁸Ramkumar, R. L., and Thaker, Y. R., "Dynamic Response of Curved Laminated Plates Subjected to Low Velocity Impact," *Journal of Engineering Materials and Technology*, Vol. 109, Jan. 1987, pp. 67–71.

⁹Christoforou, A. P., and Swanson, S. R., "Analysis of Simply-Supported Orthotropic Cylindrical Shells Subject to Lateral Impact Loads," *Journal of Applied Mechanics*, Vol. 57, June 1990, pp. 376–382.

¹⁰Bachrach, W. E., and Hansen, R. S., "Mixed Finite-Element Method for Composite Cylinder Subjected to Impact," *AIAA Journal*, Vol. 27, No. 5, 1989, pp. 632–638.

¹¹Lin, H. J., and Lee, Y. J., "Impact-Induced Fracture in Laminated Plates and Shells," *Journal of Composite Materials*, Vol. 24, Nov. 1990, pp. 1179–1199.

¹²Palazotto, A., and Perry, R., "Impact Response of Graphite/Epoxy Cylindrical Panel," *AIAA Journal*, Vol. 30, No. 7, 1992, pp. 1827–1832.

¹³Swanson, S. R., Smith, N. L., and Qian, Y., "Analytical and Experimental Strain Response in Impact of Composite Cylinders," *Composite Structures*, Vol. 18, 1991, pp. 95–108.

¹⁴Kim, S. J., and Oden, J. T., "Interior Penalty Methods for Finite Element Approximations of the Signorini's Problem in Elastostatics," *Computers and Mathematics with Applications*, Vol. 18, No. 1, 1982, pp. 36–56.

¹⁵Oden, J. T., and Carey, G. G., *Finite Elements*, Vol. V, *Special Problems in Solid Mechanics*, Prentice-Hall, Englewood Cliffs, NJ, 1984, Chap. 4.

¹⁶Kikuchi, N., and Oden, J. T., *Contact Problems in Elasticity: A Study of Variational Inequalities and Finite Element Methods*, Society for Industrial and Applied Mathematics, Philadelphia, PA, 1988, Chap. 9.

¹⁷Kim, S. J., and Kim, J. H., "Finite Element Analysis of Laminated Composites with Contact Constraint by Extended Interior Penalty Methods," *International Journal for Numerical Methods in Engineering*, Vol. 36, No. 20, 1993, pp. 3421–3439.

¹⁸Hughes, T. J. R., *The Finite Element Method—Linear Static and Dynamic Finite Element Analysis*, Prentice-Hall, Englewood Cliffs, NJ, 1987, pp. 242–250.

¹⁹Simo, J. C., and Rifai, M. S., "A Class of Mixed Assumed Strain Methods and the Method of Incompatible Modes," *International Journal for Numerical Methods in Engineering*, Vol. 29, June 1990, pp. 1595–1638.

²⁰Simo, J. C., and Armero, F., "Geometrically Non-Linear Enhanced Strain Mixed Method and the Method of Incompatible Modes," *International Journal for Numerical Methods in Engineering*, Vol. 33, May 1992, pp. 1413–1449.

²¹Goo, N. S., Kim, S. J., and Jung, S. N., "Dynamic Contact Analysis of Laminated Composite Plates Under Low-Velocity Impact," *Proceedings of the AIAA/ASME/ASCE/ASC 37th Structures, Structural Dynamics, and Materials Conference* (Salt Lake City, UT), AIAA, Washington, DC, 1996, pp. 776–786 (AIAA Paper 96-1405).

²²Oden, J. T., and Kikuchi, N., "Finite Element Methods for Constrained Problems in Elasticity," *International Journal for Numerical Methods in Engineering*, Vol. 18, May 1982, pp. 701–725.

²³Goo, N. S., "On the Dynamic Behavior and Damage Prediction of Composite Structures Under Low-Velocity Impact," Ph.D. Dissertation, Dept. of Aerospace Engineering, Seoul National Univ., Seoul, Republic of Korea, Feb. 1996.

²⁴Wu, H. T., and Springer, G. S., "Impact Induced Stresses, Strains, and Delaminations in Composite Plates," *Journal of Composite Materials*, Vol. 22, June 1988, pp. 533–560.

²⁵Carpenter, N. J., Taylor, R. L., and Katona, M. G., "Lagrange Constraints for Transient Finite Element Surface Contact," *International Journal for Numerical Methods in Engineering*, Vol. 32, No. 1, 1991, pp. 103–128.

²⁶Zhong, Z., *Finite Element Procedures for Contact-Impact Problems*, Oxford Univ. Press, New York, 1993, Chap. 9.

²⁷Kim, T. W., Goo, N. S., Yu, J. Y., and Kim, S. J., "Impact Response and Damage Analysis of Cylindrical Composite Panels," *Journal of the Korean Society for Composite Materials*, Vol. 8, No. 1, 1995, pp. 1–9 (in Korean).

²⁸Chao, C. C., and Tu, C., "Three Dimensional Contact Dynamics of Laminated Plates Impacted by Rigid Spheres," *Proceedings of Second International Conference on Composite Engineering* (New Orleans, LA), edited by D. Hui, International Community for Composite Engineering, 1995, pp. 117, 118.